JOURNAL OF Applied Polymer SCIENCE

Thermal and Mechanical Properties of Polyisobutylene-Based Thermoplastic Polyurethanes

Pallavi Kulkarni,[1] Umaprasana Ojha,[1] Xinyu Wei,[1] Niraj Gurung,[2] Kasyap Seethamraju,[2] Rudolf Faust[1]

[1]Department of Chemistry, University of Massachusetts Lowell, One University Avenue, Lowell, Massachusetts
[2]Boston Scientific Corporation, 4100 Hamline Ave North, St. Paul, Minnesota
Correspondence to: R. Faust (E-mail: Rudolf_faust@uml.edu)

ABSTRACT: We investigated thermal and mechanical properties of thermoplastic polyurethanes (TPUs) with the soft segment comprising of both polyisobutylene (PIB) and poly(tetramethylene)oxide (PTMO) diols. Thermal analysis reveals that the hard segment in all the TPUs investigated is completely amorphous. Significant mixing between the hard and soft segments was also observed. By adjusting the ratio between the hard and soft segments, the mechanical properties of these TPUs were tuned over a wide range, which are comparable to conventional polyether-based TPUs. Constant stress creep and cyclic stress hysteresis analysis suggested a strong dependence of permanent deformation on hard segment content. The melt viscosity correlation with shear rate and shear stress follows a typical non-Newtonian behavior, showing decrease in shear viscosity with increase in shear rate. © 2013 Wiley Periodicals, Inc. J. Appl. Polym. Sci. 000: 000–000, 2013

KEYWORDS: polyurethanes; thermal properties; mechanical properties

Received 24 October 2012; accepted 25 January 2013; published online
DOI: 10.1002/app.39236

INTRODUCTION

Thermoplastic polyurethanes (TPUs) are $(AB)_n$ type multiblock copolymers. The A block, also called the hard segment (HS), consists of polymer chains that are highly stiff at room temperature, and the B block, also referred to as the soft segment (SS), is polymer chains that have low glass transition temperature or melting point and thus are highly flexible at room temperature. The microphase separation between the HS and SS leads to a series of unique properties, which made TPUs important thermoplastic elastomers in a variety of applications. By adjusting the chemical structure as well as the fraction of the HS and SS, the mechanical properties of TPUs can be tailored over a wide range. However, most of the commercially available TPUs are not suitable for biomedical devices, because the SS generally consists of polyether diols, which are highly susceptible to oxidative degradations.[1–3] Such degradations substantially decrease the mechanical properties and *in vivo* lifetime of TPUs, which is a significant drawback for biomedical applications.

Polyisobutylene (PIB) is well-known for its excellent biostability and biocompatibility. Recently, the facile synthesis of PIB diol has been developed,[4–6] which allows the preparation of PIB-based TPUs (including polyureas and polyurethaneureas).[7–10] Compared with polyether-based TPUs, PIB-based TPUs exhibit significantly improved biostability.[11] However, PIB-based TPUs show much poorer mechanical performance than polyether-based TPUs,[7,9,12] which limits their potential applications. Recently, it has been demonstrated that the mechanical properties of PIB-based TPUs can be dramatically enhanced if a small amount of polyether diol, such as poly(tetramethylene oxide) (PTMO) diol, is incorporated into the SS,[8,10,13] and the biostability is still acceptable since the overall weight fraction of the polyether diol is low.[11] Especially, PIB-based TPUs containing 20 wt % of PTMO diol in the SS were found to have desirable mechanical properties, with excellent biostability and biocompatibility.[11,14]

In this article, we further investigate the thermal, mechanical and rheological properties of PIB-based TPUs containing 20 wt % of PTMO diol in the SS. A series of mechanical measurements, such as compression set, hysteresis, creep and capillary rheology were performed. Our results suggest that these TPUs have mechanical properties comparable to conventional polyether-based TPUs. Therefore, they are very promising for biomedical applications.

EXPERIMENTAL

Materials

PTMO diol (M_n = 1000 g/mol), 4,4′-methylenebis(phenyl isocyanate) (MDI) (98%), 1,4-butandiol (BDO) (99%), Tin(II) 2-

Additional Supporting Information may be found in the online version of this article.

ethylhexanoate ($Sn(oct)_2$) (95%) were purchased from Sigma-Aldrich and used as received. PIB diol (M_n = 2000 g/mol) was synthesized according to literature.[4,15] Toluene was dried over sodium and distilled.

Instrumentation

Thermogravimetric analysis (TGA) was performed on a TA Instruments Q50 thermogravimetric analyzer. Samples were heated at the rate of 10°C/min under both N_2 and air.

X-ray diffraction (XRD) measurements were performed on a Scintag XDS 2000 diffractometer. The wavelength of incident X-ray beam is 0.154 nm (Cu Kα). Diffraction signals were collected in 2θ range of 1–40°, with a scan rate of 2°/min.

Static tensile properties, tear strength and hysteresis were measured using an Instron Tensile Tester 4400R. The TPUs were compression molded into films by using a Carver Laboratory Press Model C at 180°C and a load of 16,000 lbs. The thickness of the films ranged between 0.2 and 0.3 mm. Dog-bone specimen were punched out according to ASTM D412 and pulled in the Instron at an extention rate of 50 mm/min using a 50 lbs load cell. Tear strength of the polymers was measured using ASTM D624 die C (half-size). Hysteresis tests were performed using dog-bone specimen with L_0 = 24 mm. Samples were stretched to 300% and released for five cycles at a crosshead speed of 25 mm/min. Percent hysteresis and total hysteresis were calculated by:

$$\%\ \text{hysteresis of } n\text{th cycle} = \frac{(A_{s,n} - A_{r,n})}{A_{s,n}} \times 100 \quad (1)$$

$$\%\ \text{total hysteresis after } n \text{ cycles} = \frac{(A_{s,1} - A_{r,n})}{A_{s,1}} \times 100 \quad (2)$$

where $A_{s,n}$ is the area under the stretch curve if nth cycle, $A_{s,1}$ is the area under the stretch curve of the first cycle and $A_{r,n}$ is the area under the recovery curve of nth cycle.

For compression set measurements, a Carver press was used as the compression set fixture. Two pieces of specimen with a total thickness of ~3.2 mm were used. The spacer thickness was 2.25 mm, which provided ~30% compression on the specimen. The specimens were subjected to compression for 22 h at room temperature. After that, the specimen were removed and placed aside for 1 h to recover. The thickness was then accurately measured and % compression set was determined from the following equation:

$$\%\ \text{Compression set} = \frac{(d_0 - d_1)}{d_0 - d_2} \times 100\% \quad (3)$$

where d_0 is the initial specimen thickness (mm), d_1 is final specimen thickness (mm), and d_2 is specimen thickness during compression (spacer thickness) (mm).

Dynamic mechanical analysis (DMA), creep and flexural modulus studies were performed on a TA Instruments Q800 dynamic mechanical analyzer. The TPUs were first compression molded into flat films, and the films were further cut into rectangular strips. For DMA measurements, the strips were fixed onto a film tension clamp and heated from -100 °C to 150 °C at a rate of 3°C/min and a frequency of 1Hz, and with a preload force of 0.001 N. For creep experiments, a film tension clamp was also used to hold the sample. The measurements were performed at 23°C, with a soak time of 5 min. A preload force of 0.01 N and a constant stress of 2 MPa (Viscoelastic region) were applied. A creep time of 60 min and recovery time of 20 min was used. For flexural modulus investigations, a dual cantilever clamp (20 mm span length) was fixed and calibrated. A temperature ramp/frequency sweep run was carried out at a frequency of 1 Hz and amplitude of 40 μm from −100°C to 150°C.

A Galaxy 3x Capillary Rheometer was used to determine the rheological properties of PIB-PTMO-TPUs. A melt temperature of 190°C was used. The die had a capillary of radius 0.0195 in. and length of 1.1820 in. Other parameters such as melt time, test delay, melt force and terminal force were maintained at 300 min, 5 s, 1500 lbs, and 1800 lbs, respectively. The capillary with an L/D ratio of 30 was chosen and shear rate sweep program was run from 10 (1/s) to 1000 (1/s). Polymers were dried overnight under vacuum at 60°C to remove adsorbed moisture. Approximately 3 g polymer was weighed and added to the heated cylinder and extruded out through the capillary using a shear rate sweep program with high shear rates. This facilitated cleaning of the cylinder and the capillary to remove any residual foreign material. Then 10 g polymer was weighed and charged to the rheometer. The polymer was then extruded from the capillary by using shear rates from 10 (1/s) to 1000 (1/s).

Synthesis of PIB-Based TPUs

A typical two-step synthetic procedure is as follows: To a three neck round bottom flask equipped with a mechanical stirrer, 80g PIB diol (40 mmol) and 20 g PTMO diol (20 mmol) were added and dried by azeotropic distillation using dry toluene (100 ml). To the mixture, 600 ml dry toluene was added, followed by $Sn(Oct)_2$ (0.45 g, 1.11 mmol). The mixture was then heated to 100°C and MDI (27.8 g, 111 mmol) was added. After the mixture was stirred vigorously for 30 min, BDO (4.6 g, 51 mmol) was added. The reaction mixture was further stirred for 6 h, cooled to room temperature and poured onto a Teflon mold. After the solvent had evaporated, the polymer was further dried at 50°C under vacuum overnight.

Tubing Extrusion

The TPUs were extruded on conventional single screw extruders to produce tubing and to identify nominal processing conditions. Tubing extrusion set up included a 1" single screw extruder equipped with a screen pack, a transition zone from the barrel end to the tubing die, a water bath, a laser-based online sizing sensor for outer diameter measurements, a puller and a winder. The TPU was dried at 65–75°C under vacuum until the volatile content was below 100 ppm. Extrusion was conducted at different screw speeds (5, 10, or 20 rpm), melt temperatures (185–210°C) and distances of the gap from the die head to water tank (1/8" – 3/4"). PIB-based TPU tubings with 1.7 mm outer diameter and 1.5 mm inner diameter were produced. Extruded tubings were further cured at room temperature for 3 days.

RESULTS AND DISCUSSION

Characterization of PIB-Based TPUs

Three PIB-based TPU samples were synthesized, and their characteristics are summarized in Table I. They have different weight fraction of the HS and SS, but all the samples contain 80 wt % of PIB diol and 20 wt % of PTMO diol in the SS. According to their Shore hardness, these TPUs are denoted as PIB-PTMO-TPU 60A, 80A, and 100A, respectively. For comparison, the commercially available polyether-based TPU Pellethane 55D was also investigated. Pellethane 55D has similar SS/HS ratio as PIB-PTMO-TPU 100A, but its SS consists of only PTMO diol.

Thermal Stability

Thermal stability of TPUs is very important in determining the processing conditions. Here we used TGA to study both nonoxidative and oxidative thermal stability of PIB-PTMO-TPUs. The TGA profiles are shown in Figure 1. As can be seen, in both nonoxidative and oxidative environments, the three PIB-PTMO-TPUs are thermally stable up to ~ 230–240°C, the same temperature range as Pellethane 55D. These results indicate that PIB-based TPUs have similar thermal stability as PTMO-based TPUs. Since thermal degradation of TPUs starts with degradation of the HS between 200 and 400°C and is followed by the decomposition of the SS between 400 and 500°C,[16,17] it is reasonable to see that replacing PTMO diol with PIB diol does not change the onset decomposition temperature significantly.

Thermal Properties

Recently, we performed DSC measurements on these PIB-PTMO-TPUs.[18] No endothermic peak above 200°C was observed on the second heating cycle, which suggest that the HS in all three TPUs is completely amorphous. To further confirm our DSC observation, XRD was performed on compression molded samples. As can be seen from Figure 2, all the samples show very broad and diffuse peaks arising from the amorphous polymer chains. The absence of any sharp diffraction peaks further supports our previous observation that the HS in these TPUs is highly amorphous. Previously, Koberstein et al. systematically studied the crystallization behavior of PTMO-based TPUs. Their results showed that the crystallinity was observed only when the weight fraction of HS is above 40%, and even for TPUs with much higher weight fraction of the HS, the crystallinity of the HS was still as low as ~15%.[19] Similarly, in PDMS-based TPUs containing 40 wt % of the HS, the HS was also found to be amorphous.[20] In our case, since the highest weight fraction of the HS is 40% in 100A, it is reasonable to see that the HS is completely amorphous.

In our previous DSC measurements, we could not see the glass transition of the SS very clearly, probably due to the very small

Table I. Characteristics of TPU Samples

TPU sample	Weigh fraction of the SS (%)	Weight fraction of PIB diol in the SS (%)	Shore hardness
PIB-PTMO-TPU 60A	79	80	60A
PIB-PTMO-TPU 80A	65	80	80A
PIB-PTMO-TPU 100A	60	80	100A
Pellethane 55D	60	0	100A

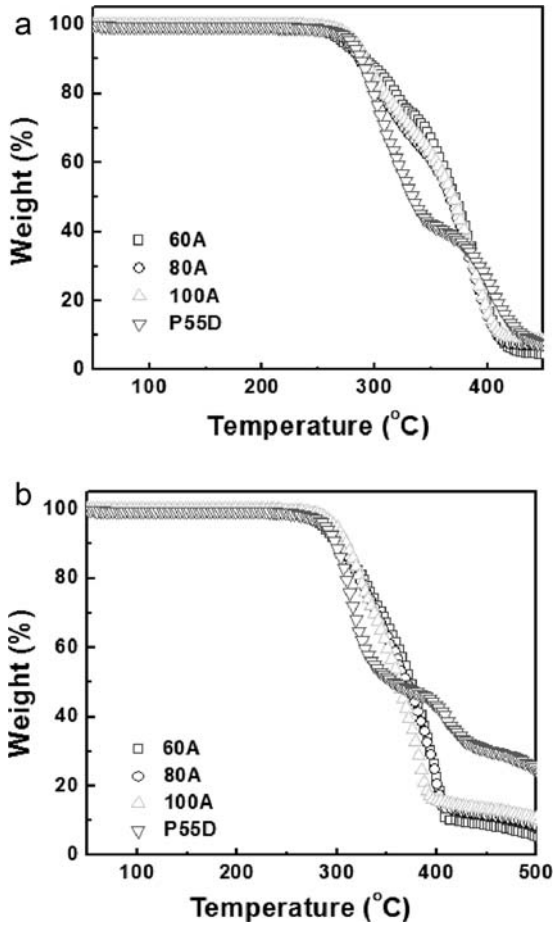

Figure 1. TGA profiles of PIB-PTMO-TPU 60A, 80A, 100A, and Pellethane 55D. The measurements were preformed in N_2 (a) and air (b), respectively.

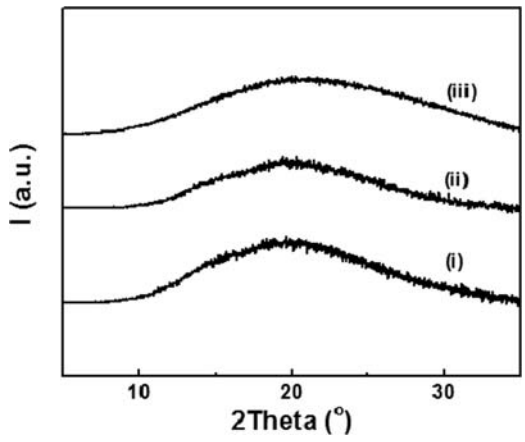

Figure 2. XRD profiles of PIB-PTMO-TPU 60A (i), 80A (ii) and 100A (iii), respectively. Profile curves are offset for clarity.

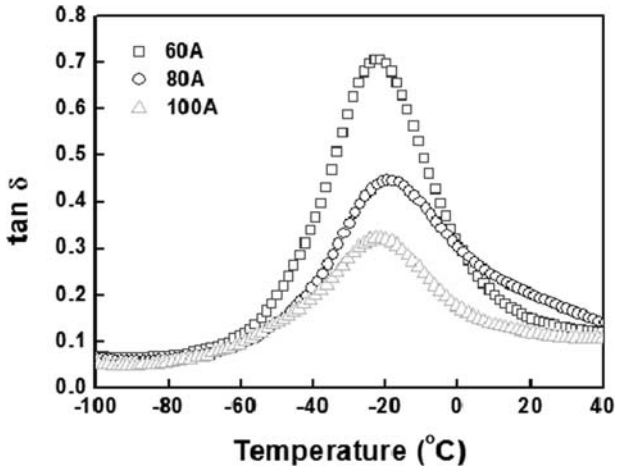

Figure 3. DMA profiles of tanδ as a function of temperature of PIB-PTMO-TPU 60A, 80A, and 100A.

change in heat capacity.[12] Therefore, we used DMA to further investigate the thermal transitions of PIB-PTMO-TPUs, since DMA is more sensitive to detect the glass transition. Figure 3 shows the plot of tan δ as a function of temperature for PIB-PTMO-TPU 60A, 80A and 100A, respectively. For all the samples, a sharp peak was observed at around −25°C, which should correspond to the glass transition of the SS. The glass transition temperature of the SS is much higher than the glass transition temperature of both PIB and PTMO homopolymers, indicating a significant mixing between the SS and HS. The glass transition temperature of the mixed PIB/PTMO soft segment in a TPU with bis(4-isocyanatocyclohexyl) methane (HMDI)/1,6-hexanediol (HDO) hard segments, reported by Erdodi et al.,[13] was also higher than both PIB and PTMO homopolymers, suggesting similar phase mixing. The fact that only one glass transition was observed also suggests that the PIB and PTMO diols did not phase separate from each other in the SS. Similar result was also reported by Mitzner et al.[9]

Static Mechanical Properties

The tensile stress at break, elongation at break, flexural modulus and compression set values of PIB-PTMO-TPU 60A, 80A, and 100A are summarized in Table II. These properties of Pellethane 55D were also measured and are listed for comparison.

As can be seen from Table II, with the hardness of these TPUs increased from 60A to 100A, the tensile stress at break increases from 20 MPa to 26 MPa, whereas the elongation at break decreases from 550 to 250%. Young's modulus of these TPUs shows much stronger dependence on the weight fraction of the HS. As can be seen, while PIB-PTMO-TPU 60A (20 wt % of HS) has a modulus of ~6 MPa and PIB-PTMO-TPU 80A (35% hard segment) has a modulus of ~15 MPa, PIB-PTMO-TPU 100A shows a sharp increase in modulus (~75 MPa). This sharp increase may be due to greater phase separation of the HS and SS. These PIB-PTMO TPUs show better ultimate tensile strength and elongation than the PIB-PTMO TPUs with the HS based on HMDI/HDO and similar compositions.[13]

Flexural modulus is an intensive property of the polymer. It measures the ability of a polymer to bend. Generally, a stiffer material shows greater resistance to bend and hence has higher flexural modulus. Pellethane 55D has the highest flexural modulus about 160 MPa. The flexural modulus values for PIB based TPUs is much lower (10–50 MPa) and increases with increase in polymer hardness. Some applications require the material to have a lower flexural modulus so that it can be bend easily without breaking. PIB-based TPUs are soft and so do not actually break under the applied load.

Compression set is the measure of the permanent deformation of the polymer when the applied stress is released. It measures the ability of the material to bounce back after stress has been applied for a prolonged period of time. Generally, softer materials are more resilient and therefore have lower compression set value. This tendency is also observed in PIB-PTMO-TPUs. As can be seen from Table II, TPU 60A shows the lowest amount of permanent set (~ 8%), TPU 80A shows a relatively higher value, around 16%, and TPU 100A has the highest value, around 30%.

Hysteresis Studies

Since biomaterials are constantly exposed to cyclic loading and unloading when they are used inside human body, the hysteresis behavior of these TPUs is crucial for long-term applications. To determine the hysteresis of PIB-based TPUs, 5 cycles, 300% hysteresis of these TPUs were investigated and compared with the results of Pellethane 55D.

Figure 4 and Supporting Information Table S1 and S2 show the cyclic hysteresis curves for Pellethane 55D and PIB-PTMO-TPU 60A, 80A, and 100A and further summarizes the values of hysteresis after each cycle. As expected, the total hysteresis increases till the third cycle and then remains almost constant. For example, the hysteresis of PIB-PTMO-TPU 60A was 61% hysteresis after the first cycle and increased to 66% after the third cycle. However, the hysteresis was 67% after the fourth and fifth cycles. The hysteresis of each individual cycle (Supporting

Table II. Summary of Mechanical Properties of TPUs

Sample	Tensile stress at break (MPa)	Elongation at break (%)	Young's modulus (MPa)	Flexural modulus (MPa)	Compression set (%)
PIB-PTMO-TPU 60A	20 ± 1	550 ± 50	6.5 ± 1	15	8
PIB-PTMO-TPU 80A	27 ± 1	475 ± 30	15 ± 2	30	16
PIB-PTMO-TPU 100A	26 ± 1.3	250 ± 25	75 ± 5	45	30
Pellethane 55D	55 ± 5	400 ± 50	25 ± 2	160	25

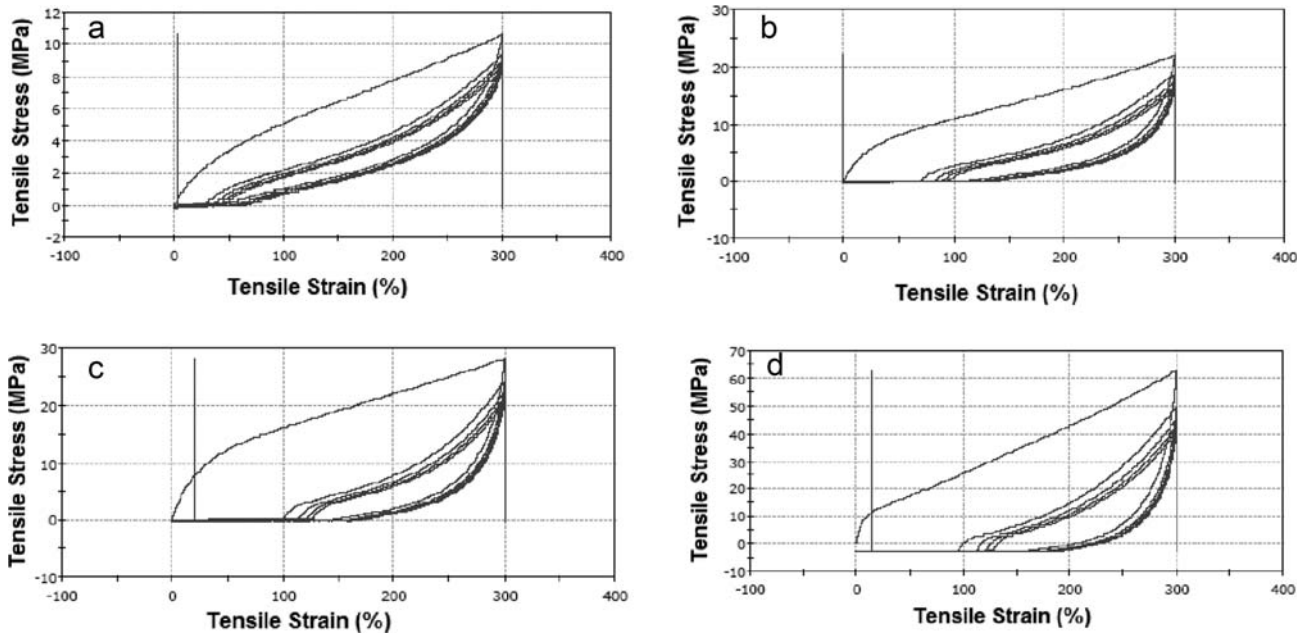

Figure 4. Strain hysteresis curves of PIB-PTMO-TPU 60A (a), 80A (b), 100A (c), and Pellethane 55D (d).

Information Table S2), on the other hand, decreases with an increase in cycles, and the maximum hysteresis was observed in the first cycle. The initial high hysteresis of PIB-PTMO-TPU 60A is due to the permanent deformation produced in the hard segment morphology. After the first cycle, the other cycles are nearly identical and display much lower hysteresis. As expected, the harder (80A and 100A) compositions show increased hysteresis due to increased deformation of the hard segments. Importantly, PIB-PTMO-TPU 100A shows somewhat lower initial and total hysteresis compared to Pellethane 55D. These findings are similar to that reported by Erdodi et al.[13] for PIB-PTMO based TPUs with HMDI/HDO hard segments of similar HS/SS compositions.

Creep Studies

Creep is defined as the time-dependent permanent deformation in a material resulting from prolonged application of constant structural stress at a constant temperature. A DMA instrument in controlled force mode (film tension clamp) was used. The creep stress was chosen in order to characterize creep behavior in the linear viscoelastic region. In general, in a creep test the total strain ε is the sum of three separate parts ε_1, ε_2, and ε_3. The ε_1 and ε_2 are the immediate elastic deformation and delayed elastic deformation, respectively, and ε_3 is the Newtonian flow. When load is removed after creep time, strain recovery occurs, which means creep recovery. The creep time and the recovery time were set to 60 and 20 min, respectively. Figure 5 is the plots of strain and creep compliance as a function of time for PIB-PTMO-TPU 60A, 80A, 100A, and Pellethane 55D.

As can be seen from Figure 5(a), instantaneous % strain ($\varepsilon_1 + \varepsilon_2$) decreases with the increase in hard segment content. PIB-PTMO-TPU 60A TPU shows maximum instantaneous strain (50%) followed by PIB-PTMO-TPU 80A TPU (~20%). PIB-PTMO 100A and P-55D with even higher hard segment content have lower % strain values, ~8% and ~5% respectively. PIB-PTMO-TPU 60A shows some delayed elastic deformation (ε_3), which increases with creep time. This suggests that there is continuous motion of polymer chains during the creep time

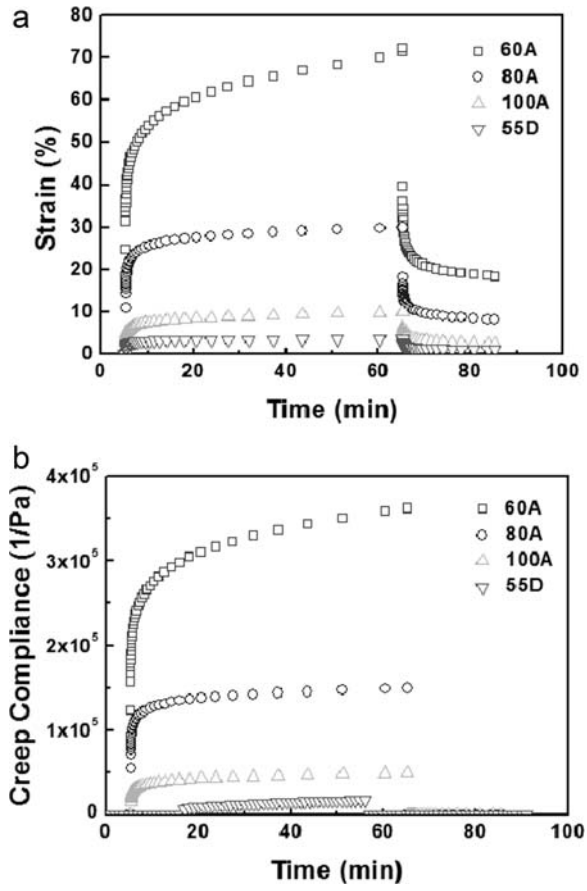

Figure 5. Plots of strain (a) and creep compliance (b) as a function of time of PIB-PTMO-TPU 60A, 80A, 100A, and Pellethane 55D.

even after instantaneous strain had occurred. PIB-PTMO-TPU 80A and TPUs with higher fraction of the HS do not show such delayed increase in strain with creep time. The hard segments restrict such delayed motion and so strain remains almost constant over the creep time.

Capillary Rheometer Studies

Melt properties of PIB-based TPUs, such as melt viscosity and melt flow rate, were determined by using a capillary rheometer. The change in shear viscosity of the polymer with change in shear rate and shear stress was determined. These plots are generally useful in designing the processing parameters of a polymer. A plot of shear viscosity as a function of shear rate was obtained [Figure 6(a)] for each polymer.

As expected, shear viscosity decreases with the increase in shear rate. The power law index (n) ranges between 1.4 and 1.7. A perfect linear correlation was observed for all the TPUs. PIB-PTMO-TPU 80A shows lower viscosity than PIB-PTMO-TPU 60A at any given shear rate value. PIB-PTMO-TPU 100A shows higher shear viscosity at the same shear rates. Processing aid such as wax may help to decrease viscosity and increase polymer melt flow. Figure 6(b) gives the correlation between shear stress and shear viscosity. The correlation of shear viscosity with shear rate and shear stress is linear for all the shear rates measured; this suggests that degradation of the urethane linkages does not take place. Lu et al.[21] studied steady state shear viscosity of 100% hard segments and concluded that degradation of urethane linkages occurs during melting of the polymer. The maximum content of hard segment in our study is 40%, which is much lower than studied by Lu et al.[21] Further, the melt temperature used in this study is 195°C, which is much lower than the minimum used in that study (210°C).

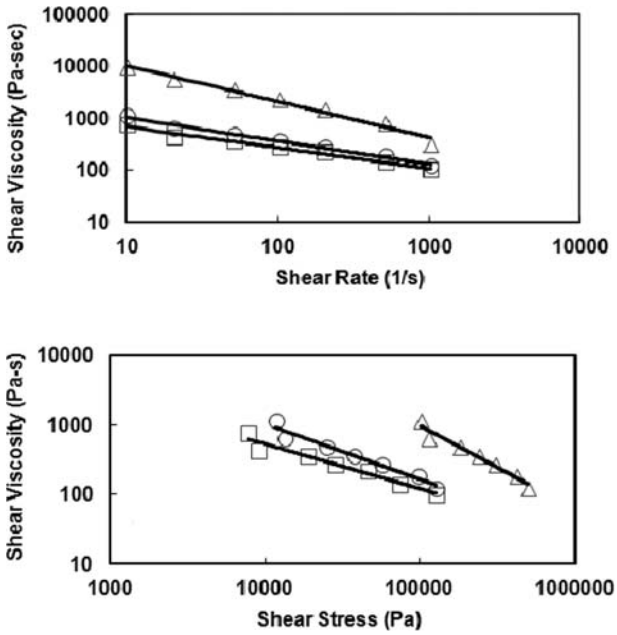

Figure 6. Plots of shear viscosity as a function of shear rate (a) and shear stress (b) of PIB-PTMO-TPU 60A(circle), 80A (square) and 100A (triangle). The solid lines are the corresponding linear fit results.

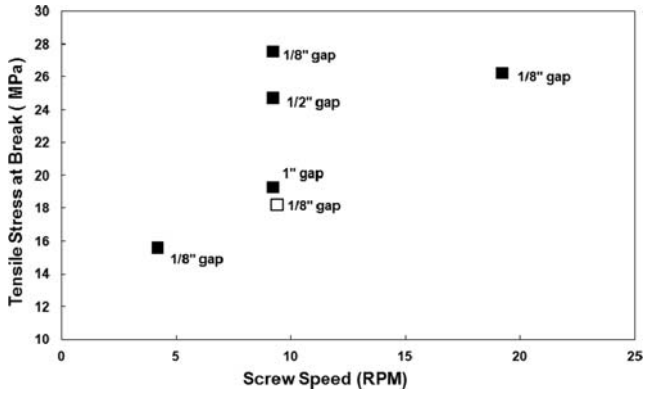

Figure 7. Plot of effects of extrusion conditions on the mechanical properties of PIB-PTMO-TPU 80A. The samples were processed at 195°C (solid symbols) and 200°C (open symbols). All the samples were annealed at 75°C for 4 h before the measurements.

Tubing Extrusion

We selected PIB-PTMO-TPU 80A to test the tubing extrusion of PIB-based TPUs. Visually clear melts out of the tubing die and clear tubings were produced at several temperatures when the melt temperatures were low, while increasing melt temperatures made the tubing color slightly whitish. As can be seen from Figure 7, tensile strength at break and elongation at break were also affected by both melt temperature and tank die gap. Our results indicated that extrusion at 195°C gives the best transparency and mechanical properties. Higher melt temperatures reduced tensile strength at break. Elongation at break values increased upon annealing the tubes at 75°C for 4 h. This suggests stress relaxation from frozen in stresses during extrusion processing. Visually clear tubing with tensile strength at break of 28 MPa and % elongation at break of 350% was produced form these experiments.

CONCLUSIONS

Thermoplastic polyurethanes based on PIB and PTMO mixed macrodiols showed good thermal and mechanical properties. Thermogravimetric analysis showed that the TPUs are thermally stable at normal elevated temperatures for processing. The tensile properties exhibited by PIB-PTMO-TPU 60A, 80A, and 100A were moderate and suitable for many applications. Furthermore, they have the ability to be tailored depending on the requirement. The impact of hard segment domains was clearly noticeable in creep, hysteresis, and compression set studies. Shear viscosity and shear rate correlations followed a power law trend and did not show any signs of degradation. This was further validated by actual extrusion of the TPUs, which produced colorless, transparent specimen. The opacity of the 100A TPU was attributed to longer hard segment lengths, which also impacted mechanical and rheological properties.

ACKNOWLEDGMENTS

This work was supported by Boston Scientific Corporation and the Massachusetts Life Sciences Center.

REFERENCES

1. Stokes, K.; McVenes, R.; Anderson, J. M. *J. Biomater. Appl.* **1995**, *9*, 321.
2. Pinchuk, L. *J. Biomater. Sci. Polym. Ed.* **1994**, *6*, 225.
3. Anderson, J. M.; Hiltner, A.; Wiggins, M. J.; Schubert, M. A.; Collier, T. O.; Kao, W. J.; Mathur, A. B. *Polym. Int.* **1998**, *46*, 163.
4. Ivan, B.; Kennedy, J. P. *J. Polym. Sci. Part A: Polym. Chem.* **1990**, *28*, 89.
5. Ojha, U.; Rajkhowa, R.; Agnihotra, S. R.; Faust, R. *Macromolecules* **2008**, *41*, 3832.
6. Ummadisetty, S.; Kennedy, J. P. *J. Polym. Sci. Part A: Polym. Chem.* **2008**, *46*, 4236.
7. Speckhard, T. A.; Gibson, P. E.; Cooper, S. L.; Chang, V. S. C.; Kennedy, J. P. *Polymer* **1985**, *26*, 55.
8. Ojha, U.; Kulkarni, P.; Faust, R. *Polymer* **2009**, *50*, 3448.
9. Mitzner, E.; Goering, H.; Becker, R.; Kennedy, J. P. *J. Macromol. Sci. Pure Appl. Chem.* **1997**, *A34*, 165.
10. Ojha, U.; Faust, R. *J. Macromol. Sci. Part A: Pure Appl. Chem.* **2010**, *47*, 186.
11. Cozzens, D.; Ojha, U.; Kulkarni, P.; Faust, R.; Desai, S. *J. Biomed. Mater. Res.* **2010**, *95A*, 774.
12. Speckhard, T. A.; Hwang, K. K. S.; Cooper, S. L.; Chang, V. S. C.; Kennedy, J. P. *Polymer* **1985**, *26*, 70.
13. Erdodi, G.; Kang, J.; Kennedy, J. P.; Yilgor, E.; Yilgor, I. *J. Polym. Sci. Part A: Polym. Chem.* **2009**, *47*, 5278.
14. Cozzens, D.; Luk, A.; Ojha, U.; Ruths, M.; Faust, R. *Langmuir* **2011**, *27*, 14160.
15. Gyor, M.; Wang, H. C.; Faust, R. *J. Macromol. Sci. Pure Appl. Chem.* **1992**, *A29*, 639.
16. Chattopadhyay, D. K.; Webster, D. C. *Prog. Polym. Sci.* **2009**, *34*, 1068.
17. Saiani, A.; Daunch, W. A.; Verbeke, H.; Leenslag, J. W.; Higgins, J. S. *Macromolecules* **2001**, *34*, 9059.
18. Cozzens, D., Wei, X., Faust, R. *J. Polym. Sci. Part B: Polym. Phys.* **2013**, *51*, 425.
19. Koberstein, J. T.; Galambos, A. F.; Leung, L. M. *Macromolecules* **1992**, *25*, 6195.
20. Choi, T.; Weksler, J.; Padsalgikar, A.; Runt, J. *Polymer* **2009**, *50*, 2320.
21. Lu, Q.-W.; Hernandez-Hernandez, M. E.; Macosko, C. W. *Polymer* **2003**, *44*, 3309.